http://dx.doi.org/10.21577/0103-5053.20180178

J. Braz. Chem. Soc., Vol. 30, No. 2, 305-309, 2019
Printed in Brazil - ©2019 Sociedade Brasileira de Química

Article

Influence of Electrooxidation of Ni Wire Electrodes on the Kinetics of Oxygen Evolution Reaction Studied in 0.1 mol dm^{-3} NaOH

Andrii Slis,[a] Tomasz Mikolajczyk[*,b] and Boguslaw Pierozynski[b]*

[a]*Department of Chemical Technology and Water Treatment, Faculty of Construction, Cherkasy State Technological University, Shevchenko Boulevard, 460, 18006 Cherkasy, Ukraine*

[b]*Department of Chemistry, Faculty of Environmental Management and Agriculture, University of Warmia and Mazury in Olsztyn, Plac Lodzki 4, 10-727 Olsztyn, Poland*

This work reports on oxygen evolution reaction (OER), studied at nickel wire electrode material. Electrocatalytic behavior of non-oxidized and electrooxidized Ni wire samples was evaluated in 0.1 mol dm^{-3} NaOH solution for the potential range: 1600-2000 mV *vs*. RHE. The performance of nickel electrodes was examined by alternating current (a.c.) impedance spectroscopy, cyclic voltammetry and Tafel polarization measurements. Electrochemical oxidation of Ni wire radically increased the kinetics of the OER, exhibited through reduced charge-transfer resistance parameter and considerably modified Tafel polarization slopes.

Keywords: nickel wire, Ni electrooxidation, OER, impedance spectroscopy

Introduction

The growth of environmental problems in regard to increasing demand for fossil fuels and energy encourages the world community to search for new energy technologies that will provide an acceptable level of pollution and, at the same time, would not slow down economic growth. According to numerous experts from all around the world, the most promising solution to this problem is the development of hydrogen-based energy.[1-3] Hydrogen is an environmentally friendly fuel, which reserves are almost inexhaustible. The above makes hydrogen a great alternative for oil and natural gas.[4,5] Water electrolysis is one of the most well-known and well-researched methods for ultra-pure hydrogen production (99.9-99.99%).[6-9]

Oxygen evolution reaction (OER) is an important part of electrolytic water splitting.[10-12] In contrast to the hydrogen evolution reaction (HER), the process of OER proceeds more slowly due to the need to transport four electrons, as compared to two electrons for the HER. For this reason, in current study the authors concentrated on the selection and development of effective catalysts for the OER, which would be characterized by low overpotentials, good performance and relatively low cost of their mass production.[3,13,14]

Nickel and its metallic compounds are widely used by different industries (e.g. Ni-Fe in metallurgy, nickel-based alloys and Ni-based superalloys are used in aviation, shipbuilding and chemical industry).[15,16] Because of its low cost, high corrosion resistance in alkaline solutions and good electrocatalytic properties, Ni and its alloys are commonly used as materials for alkaline water electrolysis and, as a result, for the production of relevant equipment.[17-21] In this paper, the OER was conducted on nickel wire (non-oxidized and electrooxidized) electrodes in 0.1 mol dm^{-3} NaOH electrolyte, primarily by means of alternating current (a.c.) impedance spectroscopy examinations.

Experimental

A Direct-Q3 UV ultra-pure water purification system from Millipore (18.2 MΩ cm water resistivity) was used to prepare all solutions. Basic solution of 0.1 mol dm^{-3} NaOH was made up from Aesar, 99.996% NaOH pellets. Additionally, a separate solution dedicated to charging of a Pd reversible hydrogen electrode was prepared from sulfuric acid of highest purity available (SEASTAR Chemicals, BC, Canada).

An electrochemical cell, made of Pyrex glass, was used during the course of this work. The cell included three electrodes: a Ni wire working electrode (WE) in a central part, a reversible Pd hydrogen electrode (RHE) as reference and a Pt counter electrode (CE), both placed in separate compartments. Before conducting the HER experiments, each Ni electrode was additionally reduced

*e-mail: tomasz.mikolajczyk@uwm.edu.pl

in 0.1 mol dm^{-3} NaOH solution by cathodic polarization at 50 mA for 600 s in order to remove any spontaneously formed Ni oxide layer. After conducting experiments on fresh nickel electrode, it was once more subjected to cathodic polarization and then was electrochemically oxidized in 0.1 mol dm^{-3} NaOH solution to examine properties of NiOOH (nickel oxyhydroxide layer) formed on its surface. Oxidation of the Ni electrode surface was carried-out by cyclic voltammetry (CV).

Cyclic voltammetry, electrochemical impedance spectroscopy and *quasi* steady-state polarization methods were used in this work. All measurements were recorded at room temperature by means of Solatron 12,608 W Full Electrochemical System. Data analysis was carried-out with ZView 2.9 (Corrview 2.9) software package, where the impedance spectra were fitted by means of a complex, non-linear, least-squares immitance fitting program LEVM 6, written by Macdonald.[22] All other experimental details, including pre-treatments applied to electrochemical cell and electrodes, and employed a.c. impedance protocol were as those given in publications by Pierozynski *et al.*;[23] Pierozynski and Mikolajczyk.[24]

Results and Discussion

Scanning electron microscopy (SEM) and energy-dispersive X-ray spectroscopy (EDS) characterization of electrooxidized Ni wire electrode

An EDS analysis was employed to determine the difference in the content of oxygen between "as received" (fresh) (Figure 1a) and oxidized (Figure 1b) Ni wire electrodes. The analysis was carried-out at an acceleration voltage of 20 kV. This experiment confirmed that the presence of oxygen in the oxidized electrode (ca. 3 wt.%) was 3× higher compared to that of the fresh electrode (ca. 1 wt.%), but due to simultaneous excitation of C element from an ultra-thin carbon tape, O assessment for both samples was rather of semi-quantitative nature. On the other hand, the SEM micrograph pictures of both electrodes did not show any visible difference between the electrodes (Figure 1c: "as received" and Figure 1d: oxidized Ni electrode).

OER on Ni wire and oxidized Ni wire electrodes in 0.1 mol dm^{-3} NaOH solution

The a.c. impedance characterization of the OER for "as received" and electrooxidized Ni wire electrodes experimentally recorded in 0.1 mol dm^{-3} NaOH is shown in Figure 2 and Table 1. For all examined potentials, both electrodes exhibited single, "depressed" semicircles (a single-step charge-transfer reaction) in the explored frequency range (examples of Nyquist impedance plots for the overpotential of 370 mV are shown in Figure 2). The electrochemical parameters (Faradic reaction resistance (R_{ct}) and double-layer capacitance (C_{dl})) were obtained by means of a constant phase element (CPE)-modified Randles equivalent circuit model (Figure 3), whereas their presentation is given in Table 1. The CPE element was used in the circuit in order to account for the capacitance dispersion effect, represented by distorted semicircles in the Nyquist impedance plots.[25-27]

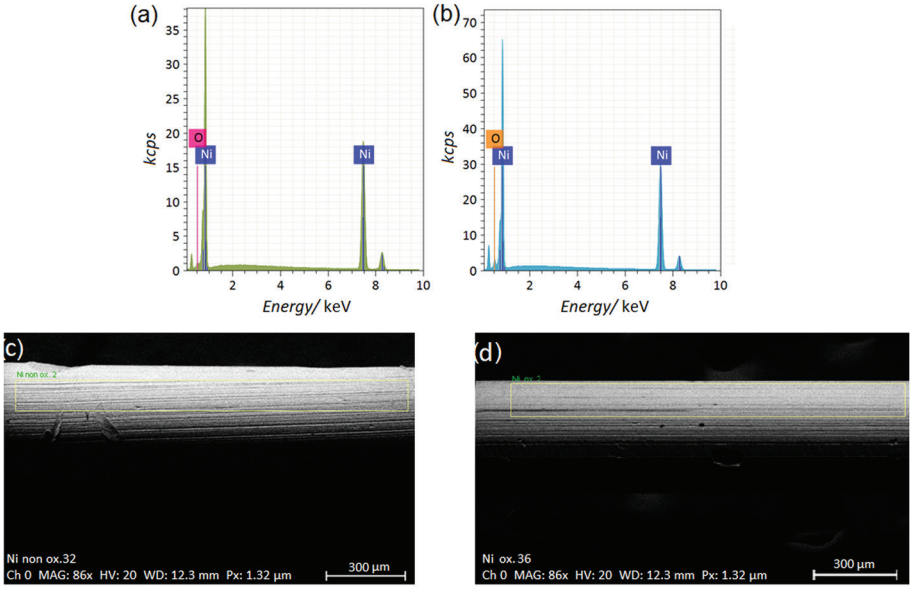

Figure 1. EDS spectrum for (a) "as received" Ni wire electrode and (b) for oxidized electrode; (c) SEM micrograph picture of (c) "as received" Ni wire electrode and (d) for oxidized Ni electrode taken at 86× magnification with visible selected area for EDS measurement.

Hence, the R_{ct} parameter for non-oxidized Ni wire electrode decreased from 6.044 Ω cm^2 at 370 mV to 0.567 Ω cm^2 at the overpotential of 770 mV. On the other hand, electrooxidation of the Ni wire electrode caused a significant fall in the R_{ct} parameter, which came to 3.874 and 0.475 Ω cm^2 at 370 and 770 mV overpotential values, respectively. Thus, the R_{ct} parameter was reduced by almost 1.6 times for the oxidized Ni wire electrode for an initial (370 mV) overpotential value (see Table 1 for details). In comparison with another important work by Hana *et al*.,[28] conducted on three dimensional (3D) nickel oxide/nickel (NiOx/Ni) electrode, the recorded R_{ct} parameter reached 4.33 and 2.46 Ω cm^2 at the overpotential of 390 mV, before and after surface oxidation, respectively. As a result, electrooxidation of nickel electrode led to the diminution of the R_{ct} parameter by ca. 1.8 times.[28]

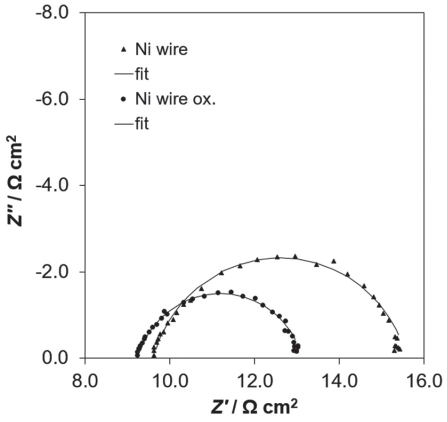

Figure 2. Complex-plane impedance plots for the OER on Ni wire and electrooxidized Ni wire electrodes in contact with 0.1 mol dm^{-3} NaOH electrolyte, recorded at room temperature for the overpotential of 370 mV. The solid lines correspond to representation of the data according to an equivalent circuit shown in Figure 3.

Table 1. Electrochemical parameters for the OER, obtained at Ni wire and oxidized Ni wire electrodes in contact with 0.1 mol dm^{-3} NaOH solution. The results were recorded by fitting the CPE-modified Randles equivalent circuit (Figure 3) to the experimentally obtained impedance data (reproducibility usually below 10-15%, $\chi^2 = 7 \times 10^{-4}$ to 1×10^{-3})

η / mV	R_{ct} / (Ω cm^2)	C_{dl} / (μF cm^{-2} s$^{\phi 1-1}$)
Ni wire		
370	6.044 ± 0.082	2,930 ± 152
470	2.001 ± 0.044	2,634 ± 256
570	1.151 ± 0.039	2,405 ± 348
670	0.720 ± 0.034	1,253 ± 334
770	0.567 ± 0.031	1,768 ± 480
Ni wire oxidized		
370	3.874 ± 0.054	4,578 ± 228
470	1.498 ± 0.031	4,038 ± 351
570	0.897 ± 0.033	4,114 ± 569
670	0.581 ± 0.025	2,717 ± 511
770	0.475 ± 0.028	4,004 ± 992

η: overpotential; R_{ct}: Faradic reaction resistance; C_{dl}: double-layer capacitance.

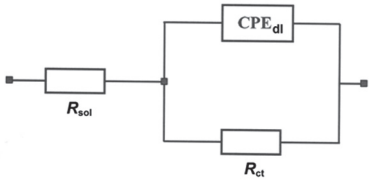

Figure 3. Equivalent circuit model used for fitting the impedance data for Ni wire electrodes, obtained in 0.1 mol dm^{-3} NaOH solution. The circuit includes a constant phase element (CPE) for distributed capacitance; R_{ct} and C_{dl} (CPE_{dl}) elements correspond to the OER charge-transfer resistance and double-layer capacitance components; R_{sol} is solution resistance.

Moreover, double-layer capacitance for both types of electrode had a tendency to somewhat decrease with rising potential. The C_{dl} value for pure Ni wire electrode reached 2,930 μF cm^{-2} s$^{\phi 1-1}$ at 370 mV and 1,768 μF cm^2 s$^{\phi 1-1}$ at 770 mV. Similarly, for electrooxidized Ni wire specimen, the C_{dl} parameter declined from 4,578 to 4,004 μF cm^{-2} s$^{\phi 1-1}$ for the corresponding overpotentials. An increase of the double-layer capacitance by about 1.6 times for the oxidized Ni wire electrode was most likely caused by the formation of NiOOH (nickel oxyhydroxide) layer on the electrode surface during the process of electrooxidation. On the other hand, the reduction of the C_{dl} parameter along with rising overpotential could be explained by partial blocking of electrochemically active electrode surface by freshly formed oxygen bubbles.[29,30]

The difference in the electrochemical performance for "as received" and the electrooxidized Ni electrodes could clearly be seen from CV data presented in Figure 4. Hence, surface-electrooxidized Ni wire exhibited significant increase of current-density within the corresponding CV profile in comparison with a baseline (fresh) electrode. In addition, an anodic peak A (Figure 4), observed between potentials 1.38 and 1.47 V *vs*. RHE for oxidized Ni wire sample, illustrated the process of formation of NiOOH from $Ni(OH)_2$, while the cathodic peak B (1.18-1.36 V *vs*. RHE) represents the reduction of nickel oxyhydroxide layer.[31]

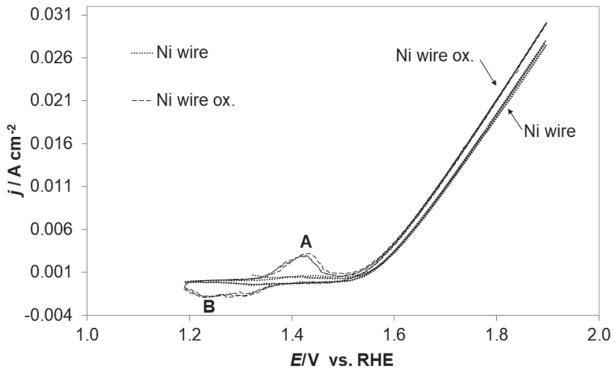

Figure 4. Cyclic voltammograms for Ni wire and electrooxidized Ni wire electrodes in contact with 0.1 mol dm^{-3} NaOH electrolyte, recorded at a sweep rate of 50 mV s^{-1} for the potential range 1.2-1.9 V *vs*. RHE.

Furthermore, a linear dependence of $-\log R_{ct}$ *vs.* overpotential (η) in Figure 5 is consistent with kinetically controlled reactions (Volmer-Heyrovski route).[32] The latter allowed to derive the OER's exchange current-densities (j_0) for these types of electrodes. The calculations were conducted by means of the Butler-Volmer equation and through utilization of the relation between the exchange current-density and the R_{ct} parameter for overpotential approaching zero value.[33,34] Hence, for the oxidized Ni wire, the recorded j_0 value for high overpotential range is almost twice as high as that for the non-oxidized Ni electrode (3.45×10^{-4} and 6.44×10^{-4} A cm^{-2}). Thus, the obtained j_0 values are quite close to those derived in other OER works. For instance, the exchange current-density values recorded for Ni-based (Ni powder, nickel plate and Co + Ni mixed oxides) electrodes in alkaline solutions ranged from 3.27×10^{-3} to 4.20×10^{-5} A cm^{-2} for high η range.[35-37]

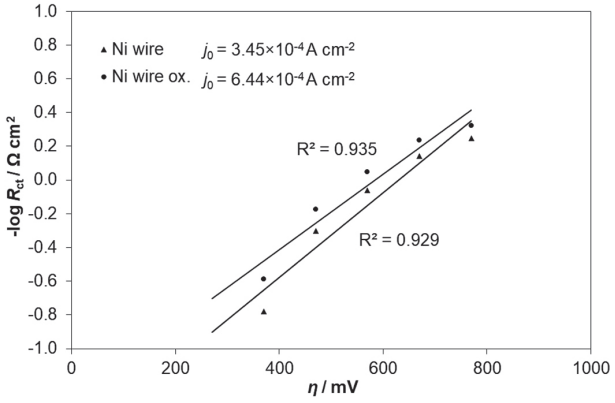

Figure 5. $-\log R_{ct}$ *vs.* overpotential relationship, obtained for the OER in 0.1 mol dm^{-3} NaOH solution for Ni wire electrodes. Symbols represent experimental results and lines are data fits.

Furthermore, the potentiostatic Tafel polarization plots are presented in Figure 6. Here, the recorded anodic slopes (b_a) approached 146 (fresh Ni wire) and 119 mV dec^{-1} (electrooxidized Ni wire) electrodes. Also, the corresponding Tafel-based j_0 parameter values for the OER came to 1.2×10^{-3} and 2.6×10^{-3} A cm^{-2} for fresh and electrooxidized Ni wire samples, respectively. However, a radical difference between the Tafel-calculated and the impedance-derived values of the j_0 parameter resulted from the fact that the linear Tafel region for the studied Ni wire electrodes was not very well pronounced. Hence, the Tafel-based data presented in this work should only be treated qualitatively.

Conclusions

Surface electrooxidation treatment was used to enhance electrochemical performance of Ni wire electrodes. It was proven that electrooxidized Ni wire catalyst was significantly more electrochemically active for the OER in regard to greater values of exchange current density than baseline Ni wire sample. In conclusion, obtained results indicated practical opportunities for electrooxidized nickel wire materials in industrial alkaline water electrolysers.

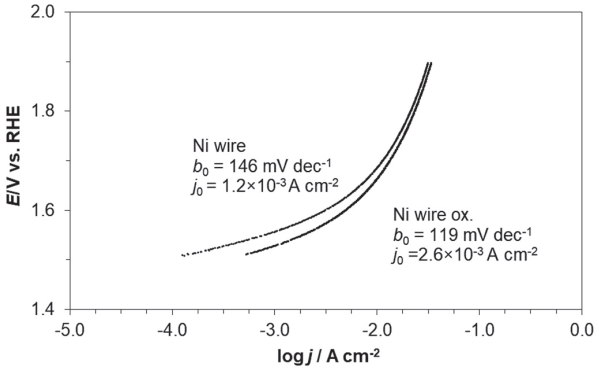

Figure 6. *Quasi*-potentiostatic anodic Tafel polarization curves (recorded at a scan-rate of 0.5 mV s^{-1}) for Ni wire and electrooxidized Ni wire electrode surfaces, carried out in 0.1 mol dm^{-3} NaOH solution (appropriate iR correction was made based on the solution resistance derived from the impedance measurements); calculated Tafel slopes for Ni wire and electrooxidized Ni wire samples came to b_a = 146 and 119 mV dec^{-1}, respectively.

Acknowledgments

This work has been financed by the internal research grant No. 20,610,001-300, provided by The University of Warmia and Mazury in Olsztyn.

References

1. Hames, Y.; Kaya, K.; Baltacioglu, E.; Turksoy, A.; *Int. J. Hydrogen Energy* **2018**, *43*, 10810.
2. Zhou, J.; Wang, C.; Lu, K.; *Int. J. Hydrogen Energy* **2016**, *41*, 16009.
3. Jiang, J.; Zhang, A.; Li, L.; Ai, L.; *J. Power Sources* **2015**, *278*, 445.
4. Qian, X.; Hang, T.; Shanmugam, S.; Li, M.; *ACS Appl. Mater. Interfaces* **2015**, *7*, 15716.
5. Zhou, M.; Weng, Q.; Popov, Z. I.; Yang, Y.; Antipina, L. Y.; Sorokin, P. B.; Wang, X.; Bando, Y.; Golberg, D.; *ACS Nano* **2018**, *12*, 4148.
6. Zeng, K.; Zhang D.; *Prog. Energy Combust. Sci*. **2010**, *36*, 307.
7. Solmaz, R.; *Int. J. Hydrogen Energy* **2013**, *38*, 2251.
8. Chakik, F.; Kaddami, M.; Mikou, M.; *Int. J. Hydrogen Energy* **2017**, *42*, 25550.
9. Solmaz, R.; Gündoğdu, A.; Döner, A.; Kardaş, G.; *Int. J. Hydrogen Energy* **2012**, *37*, 8917.
10. Lu, B.; Cao, D.; Wang, P.; Wang, G.; Gao, Y.; *Int. J. Hydrogen Energy* **2011**, *36*, 72.

11. Li, Y.; Lu, X.; Li, Y.; Zhang, X.; *Phys. E* **2018**, *99*, 1.
12. Zhou, M.; Weng, Q.; Zhang, X.; Wang, X.; Xue, Y.; Zeng, X.; Bando, Y.; Golberg, D.; *J. Mater. Chem. A* **2017**, *5*, 4335.
13. Wang, T.; Xu, W.; Wang, H.; *Electrochim. Acta* **2017**, *257*, 118.
14. Eftekhari, A.; *Mater. Today Energy* **2017**, *5*, 37.
15. Cempel, M.; Nikel, G.; *Pol. J. Environ. Stud.* **2006**, *15*, 375.
16. Kou, H.; Li, W.; Ma, J.; Shao, J.; Tao, Y.; Zhang, X.; Geng, P.; Deng, Y.; Li, Y.; Zhang, X.; Peng F.; *Int. J. Mech. Sci.* **2018**, *140*, 83.
17. Herraiz-Cardona, I.; González-Buch, C.; Ortega, E.; Pérez-Herranz, V.; García-Antón, J.; *Int. J. Chem. Mol. Eng.* **2012**, *6*, 823.
18. Vázquez-Gómez, L.; Cattarin, S.; Guerriero, P.; Musiani, M.; *Electrochim. Acta* **2008**, *53*, 8310.
19. Casas-Cabanas, M.; Hernández, J. C.; Gil, V.; Soria, M. L.; Palacín, M. R.; *J. Power Sources* **2004**, *134*, 298.
20. Goranova, D.; Lefterova, E.; Rashkov, R.; *Int. J. Hydrogen Energy* **2017**, *42*, 28777.
21. Alam, H. M. B.; Das, R.; Shajahan, M.; Ullah, A. K. M. A.; Kibria, A. K. M. F.; *Int. J. Hydrogen Energy* **2018**, *43*, 1998.
22. Macdonald, J. R.; *Impedance Spectroscopy: Emphasizing Solid Materials and Systems*; John Wiley & Sons, Inc.: New York, 1987.
23. Pierozynski, B.; Mikolajczyk, T.; Kowalski, I. M.; *J. Power Sources* **2014**, *271*, 231.
24. Pierozynski, B.; Mikolajczyk, T.; *Electrocatalysis* **2015**, *6*, 51.
25. Pierozynski, B.; Mikolajczyk, T.; *Electrocatalysis* **2016**, *7*, 121.
26. Pierozynski, B.; Smoczynski, L.; *J. Electrochem. Soc.* **2009**, *156*, B1045.
27. Conway, B. E.; Pierozynski, B.; *J. Electroanal. Chem.* **2008**, *622*, 10.
28. Hana, G. Q.; Liu, Y. R.; Hu, W. H.; Donga, B.; Li, X.; Shang, X.; Chai, Y. M.; Liu, Y. Q.; Liu, C. G.; *Appl. Surf. Sci.* **2015**, *359*, 172.
29. Kubisztal, J.; Budniok, A.; *Int. J. Hydrogen Energy* **2008**, *33*, 4488.
30. Jović, B. M.; Lačnjevac, U. Č.; Jović, V. D.; Gajić-Krstajić, Lj.; Kovač, J.; Poleti, D.; Krstajić, N. V.; *Int. J. Hydrogen Energy* **2016**, *41*, 20502.
31. Jović, B. M.; Lačnjevac, U. Č.; Jović, V. D.; Krstajić, N. V.; *J. Electroanal. Chem.* **2015**, *754*, 100.
32. Conway, B. E.; Tilak, B. V.; *Adv. Catal.* **1992**, *38*, 1.
33. Highfield, J. G.; Claude, E.; Oguro, K.; *Electrochim. Acta* **1999**, *44*, 2805.
34. Shervedani, R. K.; Madram, A. R.; *Electrochim. Acta* **2007**, *53*, 426.
35. Plata-Torres, M.; Torres-Huerta, A. M.; Domínguez-Crespo, M. A.; Arce-Estrada, E. M.; Ramírez-Rodríguez, C.; *Int. J. Hydrogen Energy* **2007**, *32*, 4142.
36. Kibria, M. F.; Mridha, M. Sh.; *Int. J. Hydrogen Energy* **1996**, *21*, 179.
37. Wu, G.; Li, N.; Zhou, D. R.; Mitsuo, K.; Xu, B. Q.; *J. Solid State Chem.* **2004**, *177*, 3682.

Submitted: June 27, 2018
Publlished online: September 13, 2018